NMR Studies of Ca^{2+} Binding to the Regulatory Domains of Cardiac and E41A Skeletal Muscle Troponin C Reveal the Importance of Site I to Energetics of the Induced Structural Changes†

Monica X. Li,‡ Stéphane M. Gagné,‡ Leo Spyracopoulos,‡ Cathelijne P. A. M. Kloks,‡ Gerald Audette,‡ Murali Chandra,§ R. John Solaro,§ Lawrence B. Smillie,‡ and Brian D. Sykes*,‡

MRC Group in Protein Structure and Function, Department of Biochemistry, University of Alberta, Edmonton, Alberta, Canada T6G 2H7, and Department of Physiology and Biophysics, College of Medicine, University of Illinois-Chicago, Chicago, Illinois 60612-7342

Received May 23, 1997; Revised Manuscript Received July 30, 1997⊗

ABSTRACT: Ca^{2+} binding to the N-domain of skeletal muscle troponin C (sNTnC) induces an "opening" of the structure [Gagné, S. M., et al. (1995) *Nat. Struct. Biol. 2*, 784−789], which is typical of Ca^{2+}-regulatory proteins. However, the recent structures of the E41A mutant of skeletal troponin C (E41A sNTnC) [Gagné, S. M., et al. (1997) *Biochemistry 36*, 4386−4392] and of cardiac muscle troponin C (cNTnC) [Sia, S. K., et al. (1997) *J. Biol. Chem. 272*, 18216−18221] reveal that both of these proteins remain essentially in the "closed" conformation in their Ca^{2+}-saturated states. Both of these proteins are modified in Ca^{2+}-binding site I, albeit differently, suggesting a critical role for this region in the coupling of Ca^{2+} binding to the induced structural change. To understand the mechanism and the energetics involved in the Ca^{2+}-induced structural transition, Ca^{2+} binding to E41A sNTnC and to cNTnC have been investigated by using one-dimensional ^1H and two-dimensional $\{^1H,^{15}N\}$-HSQC NMR spectroscopy. Monitoring the chemical shift changes during Ca^{2+} titration of E41A sNTnC permits us to assign the order of stepwise binding as site II followed by site I and reveals that the mutation reduced the Ca^{2+} binding affinity of the site I by ∼100-fold [from $K_{D2} = 16\ \mu$M [sNTnC; Li, M. X., et al. (1995) *Biochemistry 34*, 8330−8340] to 1.3 mM (E41A sNTnC)] and of the site II by ∼10-fold [from $K_{D1} = 1.7\ \mu$M (sNTnC) to 15 μM (E41A sNTnC)]. Ca^{2+} titration of cNTnC confirms that cNTnC binds only one Ca^{2+} with a determined dissociation constant K_D of 2.6 μM. The Ca^{2+}-induced chemical shift changes occur over the entire sequence in cNTnC, suggesting that the defunct site I is perturbed when site II binds Ca^{2+}. These measurements allow us to dissect the mechanism and energetics of the Ca^{2+}-induced structural changes.

Striated muscle contraction is initiated by Ca^{2+} binding to the thin filament protein TnC.[1] The resultant signal is transmitted to the other members of the thin filament (troponin I, troponin T, tropomyosin, and actin), which in turn modifies the interaction between the thick and thin filaments, leading to muscle contraction [for reviews, see Leavis and Gergely (1984), Zot and Potter (1987), Grabarek et al. (1992), Farah and Reinach (1995), and Tobacman (1996)]. Two isoforms of TnC exist in striated muscle, fast skeletal muscle TnC (sTnC) and slow skeletal/cardiac muscle TnC (cTnC). Both molecules comprise four putative EF-hand helix−loop−helix motifs as potential Ca^{2+}-binding sites (sites I−IV), except that site I in cTnC is inactive. Sites I and II are paired as a unit in the N-terminal half, and sites III and IV form another pair in the C-terminal half of the molecule. It is generally believed that the role of paired sites III and IV is structural, whereas Ca^{2+} binding to sites I and II triggers muscle contraction [see reviews listed above; also see Potter and Gergely (1975) and Szczesna et al. (1996)]. While only site II in cTnC is essential for triggering cardiac muscle contraction, both sites I and II in sTnC are required for activating fast skeletal muscle (Putkey et al., 1989; Sheng et al., 1990).

The regulatory function of sTnC is associated with a structural change induced by Ca^{2+} binding to sites I and II in the N-domain. Although the crystal structure of avian sTnC was solved a decade ago (Herzberg & James, 1988; Satyshur et al., 1988), the Ca^{2+}-induced structural transition of the N-domain remained undefined until the determination of the Ca^{2+}-bound solution structures of the intact (Slupsky & Sykes, 1995) and N-domain of sTnC (Gagné et al., 1995) using NMR spectroscopy. The structures of the N-domain in both apo and Ca^{2+}-saturated states (Gagné et al., 1995) define Ca^{2+}-induced conformational transition from a "closed" state to an "open" state. This transition involves extensive exposure of a hydrophobic patch on the surface of the molecule long proposed as the interaction site for troponin I (Herzberg et al., 1986).

The regulatory function of cTnC is associated with structural change(s) induced by Ca^{2+} binding to site II in

† Supported by the Medical Research Council of Canada, the Heart and Stroke Foundation of Canada, and the National Institutes of Health (Grant HL 49934 to R.J.S.).

* To whom correspondence should be addressed. E-mail: brian.sykes@ualberta.ca.

‡ University of Alberta.

§ University of Illinois-Chicago.

⊗ Abstract published in *Advance ACS Abstracts*, September 15, 1997.

[1] Abbreviations: TnC, troponin C; sTnC, skeletal troponin C; cTnC, cardiac troponin C; cNTnC, N-domain (residues 1−89) of recombinant human cardiac troponin C; sNTnC, N-domain (residues 1−90) of recombinant chicken skeletal troponin C; NMR, nuclear magnetic resonance; HSQC, heteronuclear single-quantum coherence; NOE, nuclear Overhauser effect; K_{D1}, dissociation constant of the first Ca^{2+} binding; K_{D2}, dissociation constant of the second Ca^{2+} binding.

S0006-2960(97)01222-1 CCC: $14.00

the N-domain. We have recently solved the solution structure of intact cTnC in the Ca^{2+}-saturated state (Sia et al., 1997) and the structures of the regulatory N-domain in both apo and Ca^{2+}-saturated states (Spyracopoulos et al., 1997). Surprisingly, it was found that unlike in sNTnC, cNTnC remains essentially closed in the Ca^{2+}-saturated state, as a consequence of the defunct site I in cTnC. We have also recently solved the solution structure of a mutant of the N-domain of sTnC (E41A sNTnC) in which the bidentate Ca^{2+} ligand Glu 41 in site I is replaced by a nonliganding residue (Gagné et al., 1997). The structure of E41A sNTnC also remains closed upon Ca^{2+} binding. Both the E41A mutant and cTnC are modified in site I, albeit differently, suggesting a critical role for this region in the direct linkage between Ca^{2+} binding and the opening of the regulatory domain.

Ca^{2+} ion chelation in a typical EF-hand involves seven liganding positions arranged as a pentagonal bipyramid. The six amino acid residues contributing to these liganding groups are designated in the sequences as positions *X*, *Y*, *Z*, $-Y$, $-X$, and $-Z$, respectively [see Strynadka and James (1989)]. In the site I of sNTnC, the Asp 30 in *X*, the Asp 32 in *Y*, and the bidentate Glu 41 in the $-Z$ position are important ligands (Strynadka et al., 1997). In cNTnC, these two aspartic acid residues are replaced by Leu and Ala residues with no Ca^{2+}-coordinating side chains. These substitutions together with the insertion of a Val residue right before the loop I in cNTnC (Van Eerd & Takahashi, 1975) cause site I to lose its Ca^{2+}-binding ability.

Although these NMR solution structures provide vital information on the end states (apo and Ca^{2+}-bound), it is important to understand the mechanism and energetics of the direct coupling between Ca^{2+} binding and induced structural changes in these regulatory domains. Previously, we have studied the Ca^{2+} binding mechanism of sNTnC by using two-dimensional (2D) $\{^1H,^{15}N\}$-HMQC NMR spectroscopy (Li et al., 1995). This approach was also applied by others to investigate Ca^{2+} binding to calbindin D_{9k} (Wimberly et al., 1995; Linse & Chanzin, 1995) and to calmodulin (Evenäs et al., 1997) and has been proven to be powerful because it can reveal information that pertains to individual atoms throughout the protein sequence. Our results demonstrated that Ca^{2+} binding to sNTnC occurs in a stepwise manner with the Ca^{2+} affinity of one site being approximately 10-fold stronger than that of the other. In this work, we used this approach to study Ca^{2+} binding to E41A sNTnC and cNTnC. During the processes of solving the NMR solution structures of E41A sNTnC and cNTnC, we have completely assigned the 2D $\{^1H,^{15}N\}$-HSQC spectra of E41A sNTnC and cNTnC in both the apo and Ca^{2+}-saturated states. These assignments are used in this paper to monitor the detailed Ca^{2+} titrations of E41A sNTnC and cNTnC. The results are used to evaluate the effect of the E41A mutation on the Ca^{2+} affinities of sites I and site II in sNTnC and on the Ca^{2+} binding energetics. Comparison of the Ca^{2+} binding properties of E41A sNTnC and cNTnC allows us to understand further the differences between slow/cardiac and fast skeletal muscle contraction.

EXPERIMENTAL PROCEDURES

Nomenclature of Proteins and Mutants. The sequence numbering of chicken recombinant sTnC differs at two positions from that of human recombinant cTnC. The first residue in cTnC corresponds to residue 3 in sTnC, and there is a valine insertion at position 28 of the cTnC sequence. Following this numbering scheme, residue 90 in sTnC corresponds to residue 89 in cTnC. The designation sNTnC (1−90) is for the fragment encompassing residues 1−90 of chicken recombinant sTnC. E41A sNTnC (1−90) describes the same fragment in which Glu 41 is mutated to Ala. The designation cNTnC (1−89) is for the fragment encompassing residues 1−89 of human recombinant cTnC.

Construction of TnC Mutants, Protein Isolation, and NMR Sample Preparation. The engineering of the expression vector of E41A sNTnC (1−90) mutant was as described for sNTnC (Gagné et al., 1994), except the pTZ18·E41A sTnC plasmid was used as a template in the polymerase chain reaction (PCR) procedures. For the preparation of pTZ18·E41A sTnC, the 1.2 kb *Eco*RI DNA fragment carrying the sTnC gene was isolated from the pLcIIFx·sTnC (Reinach & Karlsson, 1988) and subcloned into the *Eco*RI site of pTZ18 plasmid DNA (Mead et al., 1986) to give pTZ18·sTnC. Clones carrying the insert in the right orientation were identified by single-stranded DNA sequencing. To isolate uracil-containing single-stranded DNA as the template for site-specific mutagenesis, pTZ18·sTnC plasmid DNA was transformed into *Escherichia coli* CJ 236 (ung^-, dut^-) cells (Kunkel et al., 1987). The nucleotide sequence of the mutagenesis primer was 5′-CACCAAGGCGTTGGGCA-3′. The underlined nucleotides were designed to substitute Ala for Glu at position 41 of sTnC. The mutagenesis mixture was transformed into *E. coli* JM109 (ung^+, dut^+) cells. Single-stranded DNA from several clones was isolated, and the E41A mutation was confirmed by DNA sequencing. The engineering of the expression vector of cNTnC (1−89) was as described by Chandra et al. (1997).

The expressions of E41A sNTnC, [^{15}N]E41A sNTnC, cNTnC, and [^{15}N]cNTnC in *E. coli* were as described previously for sNTnC and [^{15}N]sNTnC (Gagné et al., 1994; Li et al., 1995). Purification of the proteins followed the previously published procedure for cleaved TnC (Golosinska et al., 1991). Decalcification of E41A sNTnC, [^{15}N]E41A sNTnC, cNTnC, and [^{15}N]cNTnC and their NMR titration sample preparations were as described for sNTnC (Li et al., 1995). All the NMR samples were in a 500 μL volume. The buffer conditions were 100 mM KCl and 10 mM imidazole in 90% H_2O/10% D_2O for all the E41A sNTnC NMR samples and were the same for all the cNTnC NMR samples except there was 15 mM dithiothreitol (DTT) in the buffer; the pH was 6.70. The concentrations of [^{15}N]E41A sNTnC, [^{15}N]cNTnC, and cNTnC NMR titration samples were determined to be 2.08, 1.60, and 2.50 mM, respectively, by amino acid analyses. The concentration of the [^{15}N]E41A sNTnC sample used for T_2 measurements was determined to be 1.16 mM by amino acid analyses.

Ca^{2+} Titrations of [^{15}N]E41A sNTnC, cNTnC, and [^{15}N]-cNTnC Monitored by 1D and 2D $\{^1H,^{15}N\}$-HSQC Spectra. A stock standardized 50 mM $CaCl_2$ solution and a stock 1 M $CaCl_2$ solution in water were used for the titrations. A 10 μL Hamilton syringe was used for all the $CaCl_2$ solution additions. For the titration of [^{15}N]E41A sNTnC, aliquots of 2, 3, 3, 3, 3, 4, 4, 4, 4, 5, 5, 5, 8, and 10 μL of 50 mM $CaCl_2$ were added consecutively to the NMR tube for 14 individual titration points, and a 3 μL sample of 1 M $CaCl_2$ was added for the last titration point. The total volume

changed from 500 μL before titration to 566 μL after titration. Both 1D and 2D {^{1}H,^{15}N}-HSQC spectra were acquired at every titration point. For the titration of [^{15}N]cNTnC, aliquots of 2, 3, 3, 3, 4, 4, 4, 4, 5, and 10 μL of 50 mM $CaCl_2$ were added consecutively to the NMR tube for 10 individual titration points. The total volume increase was 42 μL. Only 2D {^{1}H,^{15}N}-HSQC spectra were acquired during this titration. We performed 1D NMR titration of cNTnC separately by adding aliquots of 2, 2, 3, 3, 3, 3, 4, 5, 5, 5, 5, 10, 10, 10, and 10 μL of a 50 mM $CaCl_2$ solution consecutively to the cNTnC NMR sample with a total volume change of 80 μL. The changes in protein and Ca^{2+} concentrations due to dilutions were taken into account for data analyses. Changes in pH associated with $CaCl_2$ additions were negligible.

T_2 Measurements As Monitored by 1D NMR Spectra. A jump and return spin echo pulse sequence (Anglister et al., 1993) was used to determine the effective rotational correlation time τ_{ROT} for the protein E41A sNTnC. τ_{ROT} is proportional to the molecular weight; $\tau_{ROT} = (^4/_3\pi r^3)(\eta/kT)$. To a 500 μL sample of E41A sNTnC were added consecutively aliquots of 1, 1, 1, 1, 1, 1, 1, 2, 2, 2, 2, 2, 2, 2, 2, 2, 2, and 2 μL of 50 mM $CaCl_2$. At every point, the T_2 was measured for the envelope of the NH resonances by using $1/T_2 = \pi\Delta\nu$ and τ_{ROT} calculated from $\tau_{ROT} = {}^1/_5T_2$ (Anglister et al., 1993). The temperature was 30 °C.

NMR Spectroscopy. All 1D and 2D {^{1}H,^{15}N}-HSQC spectra were recorded on a Varian VXR-500 NMR spectrometer. The 1D spectra were acquired using a spectral width of 7000 Hz, a pulse width of 9.8 μs (90°), and an acquisition time of 2 s. The 2D {^{1}H,^{15}N}-HSQC spectra were acquired using the modified pulse scheme of Bodenhausen and Reuben (1980) with spin lock water suppression as described in Messerle et al. (1989). The temperature for all the experiments was 30 °C. Each 2D spectrum was collected with 512 complex data points in the t_2 dimension and 64 complex data points in t_1; eight transients per FID were recorded. The ^{1}H and ^{15}N sweep widths were 7000 and 1500 Hz, respectively. The 2D {^{1}H,^{15}N}-HSQC spectra were processed using the software package NMRPipe (Delaglio et al., 1995) and peak-picked using the program PIPP (Garrett et al., 1991).

RESULTS

Ca^{2+} Titration of E41A sNTnC. A series of 1D ^{1}H NMR spectra, depicting the 8.8−11 ppm region of the spectrum, during the Ca^{2+} titration of [^{15}N]E41A sNTnC are shown in Figure 1A. The two resonances near 10.3 ppm correspond to G35 and G71 (Gagné et al., 1997). The resonances for both amide NH protons appear as doublets due to coupling to the ^{15}N. The chemical shift of these resonances changes as a function of the fraction of saturation of the protein with Ca^{2+} (Figure 2). In addition, these signals start as sharp resonances, undergo a slight line broadening, and then sharpen as the $[Ca]_{total}/[E41A\ sNTnC]_{total}$ ratio is increased, indicating that the Ca^{2+} exchange kinetics fall between the intermediate and fast exchange limit on the NMR time scale (Li et al., 1995). The distinct shape of the Ca^{2+} binding plot (Figure 2A) for G35 clearly indicates the stepwise binding of Ca^{2+} to E41A sNTnC. The fact that the plot for G35 (Figure 2A) does not level off when the $[Ca]_{total}/[E41A\ sNTnC]_{total}$ ratio reaches 2 demonstrates that site I binds Ca^{2+} with a weaker affinity. On the other hand, G71 in site II is mainly affected by the binding of the first equivalent of Ca^{2+} (Figure 2B).

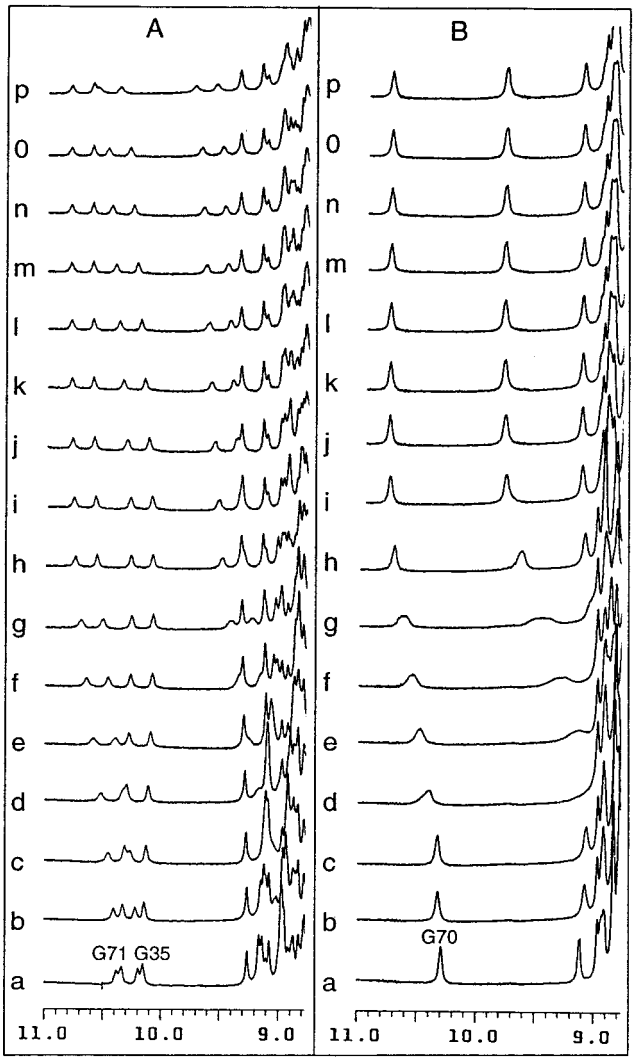

FIGURE 1: 500 MHz ^{1}H NMR spectra of 2.08 mM uniformly ^{15}N-labeled E41A sNTnC (A) and 2.5 mM cNTnC (B), shown at $[Ca]_{total}/[E41A\ sNTnC]_{total}$ ratios of (a) 0.000, (b) 0.051, (c) 0.208, (d) 0.376, (e) 0.526, (f) 0.677, (g) 0.885, (h) 1.094, (i) 1.302, (j) 1.511, (k) 1.771, (l) 2.037, (m) 2.298, (n) 2.715, (o) 3.235, and (p) 6.119 and $[Ca]_{total}/[cNTnC]_{total}$ ratios of (a) 0.000, (b) 0.027, (c) 0.114, (d) 0.244, (e) 0.374, (f) 0.505, (g) 0.635, (h) 0.809, (i) 1.026, (j) 1.243, (k) 1.460, (l) 1.677, (m) 2.112, (n) 2.546, (o) 2.980, and (p) 3.415. Conditions are described in Experimental Procedures.

Virtually all residues of E41A sNTnC (except M1, D2, D3, T4, P53, and I73) can be observed in the 2D {^{1}H,^{15}N}-HSQC spectra. The 2D {^{1}H,^{15}N}-HSQC spectra acquired during Ca^{2+} titration were well-resolved at every titration point and have been completely assigned [see Gagné et al. (1997) and Figure S1 of the Supporting Information]. The cross-peaks shifted in the ^{1}H and/or ^{15}N dimensions during Ca^{2+} titration. These chemical shift changes were plotted as a function of the $[Ca]_{total}/[E41A\ sNTnC]_{total}$ ratio (see Figure S3 of the Supporting Information), as in the case of 1D titration. All of these Ca^{2+} binding curves were fitted individually to the equation

$$P + Ca \leftrightarrows PCa + Ca \leftrightarrows PCa_2$$

with K_{D1} and K_{D2} as the macroscopic dissociation constants for the binding of the first (site II) and second (site I) Ca^{2+}

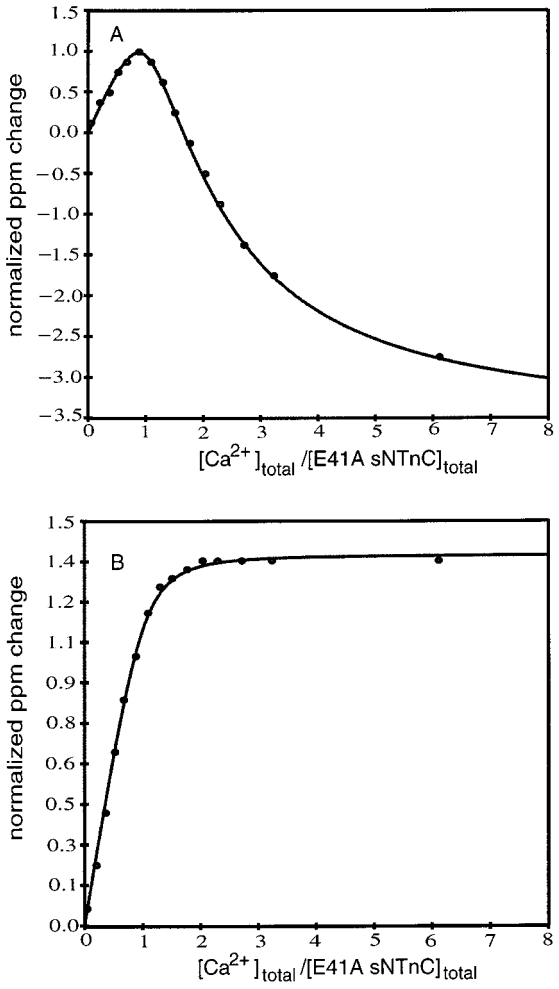

FIGURE 2: Calcium titration plots for G35 (A) and G71 (B) of E41A sNTnC derived from Figure 1A. The curve is normalized according to $(\delta_{obs} - \delta_{initial})/(\delta_{1Ca^{2+}} - \delta_{initial})$. The curves which best fit the data points are shown by the solid lines. The fitted results are shown in Results.

ions (Williams et al., 1985; Li et al., 1995). The fitting yielded a K_{D1} of 15 ± 5 μM and a K_{D2} of 1.3 ± 0.5 mM. The resultant fitted curves for G35 and G71 are shown in Figure 2.

The plots of the absolute value of the difference of the amide ^{1}H and ^{15}N chemical shifts for each residue between the apo and one-Ca^{2+}, and one-Ca^{2+} and two-Ca^{2+} states, are shown in Figure 3. Chemical shift changes occur throughout the sequence when the $[Ca]_{total}/[E41A\ sNTnC]_{total}$ ratio goes from 0 to 1, indicating that 1 equiv of Ca^{2+} is sufficient to induce global changes in this protein. Further chemical shift changes, also distributed throughout the sequence, occur when the second Ca^{2+} is added. This demonstrates that changes induced by Ca^{2+} binding to either site of E41A sNTnC are propagated globally. The most perturbed amides are those located in the two Ca^{2+} binding loops. These plots show clearly that loop II is more affected than loop I by binding the first Ca^{2+}, whereas the second Ca^{2+} induces more changes in loop I than in loop II. Taken together, these results show that the E41A mutation reduced the Ca^{2+} binding affinity of site I in sNTnC by about 100-fold ($K_{D2} \approx 16$ μM to 1.3 ± 0.5 mM, see Table 1) and of site II by about 10-fold (from $K_{D1} \approx 1.7$ μM to 15 ± 5 μM, see Table 1).

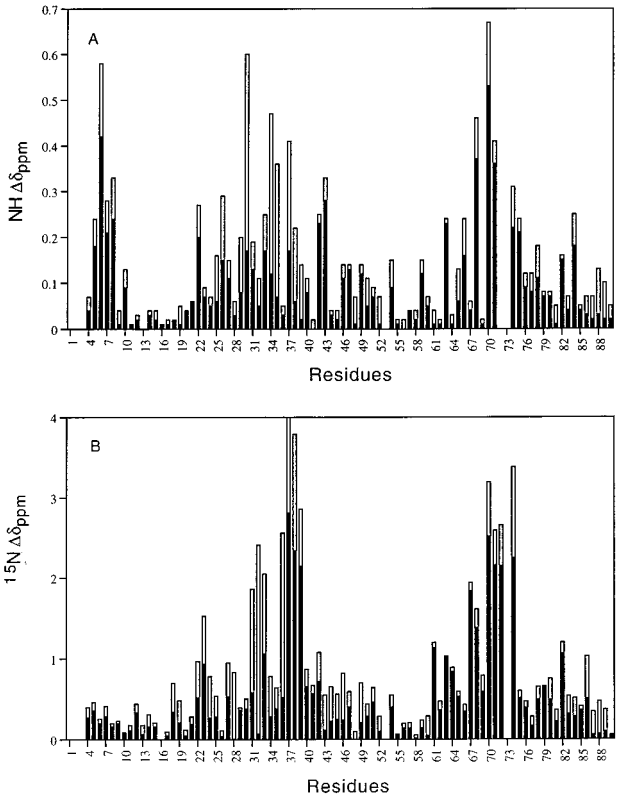

FIGURE 3: Plots of chemical shift changes (absolute values) for [^{15}N]E41A sNTnC: (A) the apo to one-Ca^{2+} state (black bar) and additional changes after the one-Ca^{2+} state (open bar) for NH and (B) the apo to one-Ca^{2+} state (black bar) and additional changes after the one-Ca^{2+} state (open bar) for ^{15}N.

Table 1: Ca^{2+} Binding Parameters for sNTnC, E41A sNTnC, and cNTnC[a]

	sNTnC[b]	E41A sNTnC	cNTnC
K_{D1} (μM)[c]	1.7 ± 1.0	15 ± 5	2.6 ± 0.1
K_{D2} (μM)[d]	16 ± 10	1300 ± 500	
$\Delta G°_1$ (kcal mol^{-1})	8.1	6.7	7.7
$\Delta G°_2$ (kcal mol^{-1})	6.9	4.1	

[a] The binding constants were obtained as described in Results. The free energy was calculated from the standard relationships $\Delta G°_1 = RT \ln K_{D1}$ and $\Delta G°_2 = RT \ln K_{D2}$. [b] Data taken from Li et al. (1995). [c] Dissociation constants for the first Ca^{2+} bound (i.e., stronger site, which has been assigned to site II). [d] Dissociation constants for the second Ca^{2+} bound (i.e., weaker site, which has been assigned to site I).

Ca^{2+} Titration of cNTnC. Ca^{2+} titration of cNTnC was also monitored using both 1D ^{1}H and 2D {^{1}H,^{15}N}-HSQC spectra. A series of 1D ^{1}H NMR spectra from the Ca^{2+} titration of cNTnC are shown in Figure 1B. The resonance at 10.3 ppm is G70 (Spyracopoulos et al., 1997), which is located in site II and corresponds to G71 in the sNTnC sequence. The chemical shift changes of this resonance are plotted as a function of the $[Ca]_{total}/[cNTnC]_{total}$ ratio as shown in Figure 4. The plot saturates at a $[Ca]_{total}/[cNTnC]_{total}$ ratio of 1, indicating that cNTnC binds only 1 equiv of Ca^{2+}. The 2D {^{1}H,^{15}N}-HSQC spectra were very well-resolved, and the spectra in apo and Ca^{2+}-saturated states are completely assigned [see Spyracopoulos et al. (1997) and Figure S2 of the Supporting Information]. All the residues along the cNTnC sequence except M1, D2, P52, and P54 were followed by ^{1}H and/or ^{15}N chemical shift changes. All the resonances in the spectra were completely

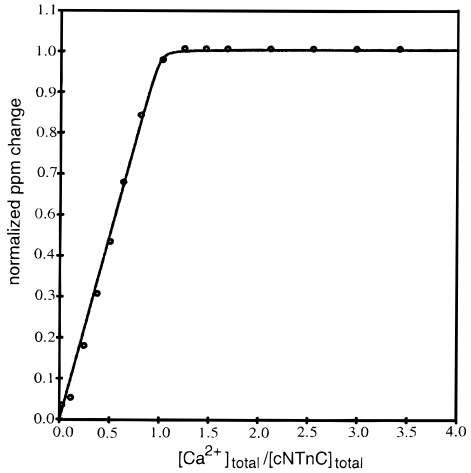

FIGURE 4: Calcium titration plot of G70 of cNTnC derived from Figure 1B. The curve is normalized according to $(\delta_{obs} - \delta_{initial})/(\delta_{1Ca^{2+}} - \delta_{initial})$. The curve which best fits the data points is shown by the solid line. The fitted results are shown in Results.

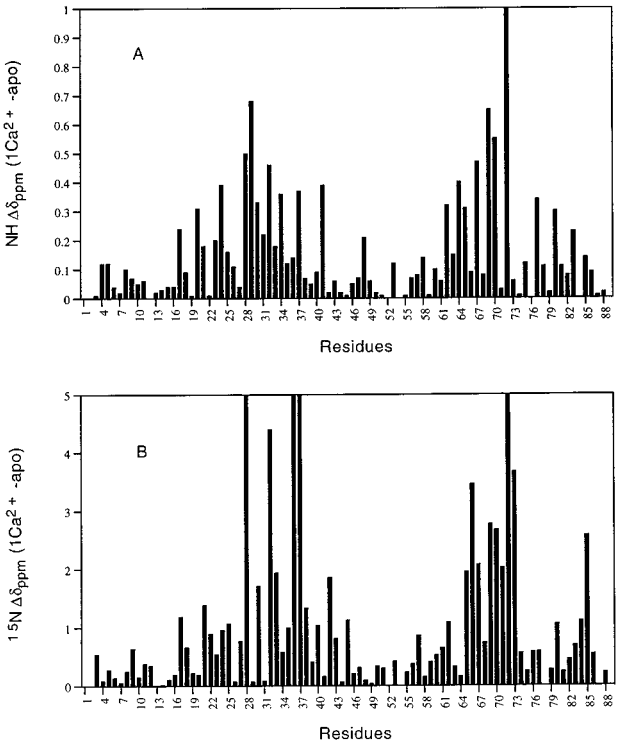

FIGURE 5: Plots of chemical shift changes (absolute values) for [^{15}N]cNTnC: (A) the apo to one-Ca^{2+} state (black bar) for NH and (B) the apo to one-Ca^{2+} state (black bar) for ^{15}N.

saturated when the $[Ca]_{total}/[cNTnC]_{total}$ ratio reached 1. The data for all amides were fitted to the equation

$$P + Ca \Leftrightarrow PCa$$

(Williams et al., 1985) and yielded a macroscopic dissociation constant K_D of 2.6 ± 0.1 μM, which agrees with the Ca^{2+} affinity of site II in the native protein ($K_D = 1-5\ \mu$M; Hannon et al., 1992; Johnson et al., 1980; Holroyde et al., 1980). Although only site II binds Ca^{2+}, the chemical shift changes are distributed all along the sequence as shown in Figure 5, which plots the absolute chemical shift change differences for both amide ^{1}H and ^{15}N for each residue. Figure 5 shows that most of the conformational perturbations by Ca^{2+} are located in the two Ca^{2+} binding loops and that, while site I is defunct, it responds to Ca^{2+} binding to site II.

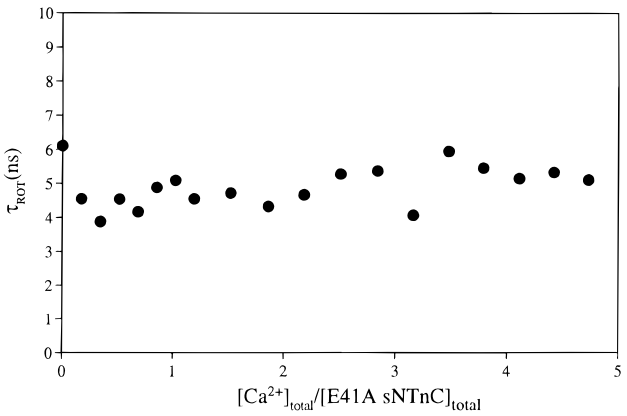

FIGURE 6: Plot of the effective rotation correlation time of E41A sNTnC determined from ^{1}H jump and return echo measurements of NH proton transverse relaxation at various $[Ca]_{total}/[E41A\ sNTnC]_{total}$ ratios.

T_2 Measurements of E41A sNTnC. The rotational correlation time (τ_{ROT}) for the protein is proportional to its molecular weight, and also is influenced by the aggregation state of the protein. Figure 6 shows the τ_{ROT} values determined for E41A sNTnC during the Ca^{2+} titration, which vary in the range of 5.0 ± 1.1 ns corresponding to a molecular weight range of 7800−12200 with a median value of 10000, which is the molecular weight of E41A sNTnC (Sykes et al., 1996). This indicates that E41A sNTnC remains as a monomer upon Ca^{2+} binding in solution, unlike wild-type sNTnC (Gagné et al., 1995; Slupsky et al., 1995). The narrowness of the NMR line width and the resolution among the cross-peaks in the 2D {^{1}H,^{15}N}-HSQC NMR spectra during Ca^{2+} titration also indicate a lack of Ca^{2+}-induced aggregation/dimerization of E41A sNTnC in solution. The 2D {^{1}H,^{15}N}-HSQC spectra of [^{15}N]cNTnC acquired during the Ca^{2+} titration are comparable to those of [^{15}N]E41A sNTnC in terms of line width and resolution demonstrating no perceptible aggregation for cNTnC.

DISCUSSION

Activation of fast skeletal muscle involves binding of Ca^{2+} to two sites in the N-domain of sTnC, but only a single site in the N-domain of cTnC (Putkey et al., 1989; Sheng et al., 1990). To understand the differences in Ca^{2+} signaling between fast skeletal and cardiac muscle contraction, it is essential to have a thorough understanding of Ca^{2+} binding to the N-domains of the TnCs. We have previously studied in detail the mechanism of Ca^{2+} binding to the regulatory domain of wild-type skeletal TnC by 1D and 2D NMR spectroscopy (Li et al., 1995), and we have concluded that Ca^{2+} binding to the wild-type N-domain occurs in a stepwise manner with one site binding Ca^{2+} about 10 times stronger than the other; however, the data did not permit us to unambiguously assign the low- and high-affinity sites to structural sites I and/or II, respectively. On the basis of the amino acid residues occupying the liganding positions in site I and site II of sNTnC, we argued that site II is the site filled first. This conclusion has recently gained strong support from an analysis of the X-ray structure of sNTnC in the Ca^{2+}-bound state (Strynadka et al., 1997). Site I consists of residues **D**A**D**G**G**G**DI**STK**E**, with six potential Ca^{2+}-coordinating liganding residues as bold letters. Positions 1 and 3 are two Asps coordinating directly to Ca^{2+}, and position 12 consists of a Glu using both carboxylate oxygens

to coordinate to Ca^{2+}; position 7 involves ligand formation with the main chain carbonyl group, and positions 5 and 9 involve water molecules coordinating to Ca^{2+}. On the other hand, site II consists of residues **D**E**D**G**S**G**T**I**D**F**E**E. In comparison to site I, the Ser in position 5 interacts directly with Ca^{2+} through its O^{γ} atom. Thus, the main difference between the coordination of the Ca^{2+} ion is the fact that two water molecules are involved in site I but only one is involved in site II. In general, the more water ligands in the Ca^{2+} binding sites, the weaker the apparent Ca^{2+} affinity (Strynadka & James, 1989). In addition to the one more water molecule in site I, there is the presence of the conformationally flexible glycine triplet, the less overall negative charge for attracting Ca^{2+} ion, and the lower observed number of stabilizing hydrogen bonds (Strynadka et al., 1997). All these factors together would suggest that site I is energetically (both entropically and enthalpically) less favorable in binding Ca^{2+} than site II. This would explain that the greater Ca^{2+} binding free energy for site II ($\Delta G° = -8.1$ kcal mol^{-1}) with respect to site I ($\Delta G° = -6.9$ kcal mol^{-1}) (see Table 1). By examining the Ca^{2+}-induced conformational changes in site II, Strynadka et al. (1997) have suggested that site II is more "pre-formed" for binding Ca^{2+} than site I in terms of ligand position and hydrogen bonding interactions, which would suggest that less conformational changes may be involved in Ca^{2+} binding to site II than to site I.

Gagné et al. (1997) have suggested that ligands in site I are essential in the coupling of Ca^{2+} binding to sites I and II in sNTnC to the induced structural change. In the E41A mutant, the bidentate ligand Glu 41 (position 12) in site I is replaced by an Ala. The structure of E41A sNTnC in the Ca^{2+}-bound state remains closed, indicating that the direct linkage between calcium binding and the resultant opening of the structure is broken. On the basis of the new data reported here, we can now suggest that Ca^{2+} binding to sNTnC may involve the following steps. The first Ca^{2+} binds to site II, causing only minor structural changes and setting the stage for Ca^{2+} binding to site I , and then the second Ca^{2+} fills site I, inducing large conformational changes and the opening of the structure (Gagné et al., 1997). It should be noticed here that we have previously observed that Ca^{2+} binding to site II induced more significant far-UV CD ellipticity changes than binding to site I (Li et al., 1995), which, however, may not be directly related to the structural changes as discussed in Gagné et al. (1994). The opening of the structure and the exposure of the hydrophobic patch are energetically unfavorable in water. The energy barrier is estimated to be about 2.0 kcal mol^{-1} by a recent low-temperature, high-pressure study on sTnC (Foguel et al., 1996). In this paper, we found that site I is destabilized by 2.8 kcal mol^{-1} (from -6.9 to -4.1 kcal mol^{-1} , see Table 1) with respect to Ca^{2+} binding due to the E41A mutation. This suggests that, when site I is altered by an E41A mutation, the reduction in Ca^{2+} binding free energy roughly compensates for the energetic barrier ($\Delta G° = \sim 2.0$ kcal mol^{-1}) to open the structure and expose the hydrophobic surface. These measurements quantitatively support our conclusion (Gagné et al., 1997) that the opening of the sNTnC structure is dependent on one amino acid, Glu 41.

The present results also show that the E41A mutation destabilizes Ca^{2+} binding to site II by 1.4 kcal mol^{-1} (from -8.1 to -6.7 kcal mol^{-1} , see Table 1). Although unexpected, this result is not surprising in light of the structural coupling between the two sites. The disposition of the two EF-hands and the central β-sheet connecting them in the N-domain of sTnC is characterized well in the crystal structures with the N-domain in apo states (Herzberg & James, 1988; Satyshur et al., 1988) and in the recent Ca^{2+}-bound structure of sNTnC (Strynadka et al., 1997). These studies suggest numerous hydrogen bonding and van der Waals interactions between the two sites, especially between the two β-strands connecting site I and site II. In the NMR structure studies of Ca^{2+}-saturated sTnC (Slupsky & Sykes, 1995), sNTnC in apo and Ca^{2+}-saturated state (Gagné et al., 1995), and E41A sNTnC in the Ca^{2+}-bound state (Gagné et al., 1997), a large number of NOE contacts between the two sites were also observed. In the Ca^{2+} titration of sNTnC, we have observed that Ca^{2+} binding to either site II or site I causes chemical shift changes in both EF-hands (Li et al., 1995), suggesting widespread effects on conformational changes by each Ca^{2+} binding. In this work, we observed similar chemical shift changes for E41A sNTnC (Figure 3). In E41A sNTnC, the chemical shift changes are larger in site II for the binding of the first Ca^{2+} and larger in site I for the second Ca^{2+} clearly defining the order of the stepwise binding.

Mutating Glu to a nonbidentate ligand such as Gln or a nonligand such as Ala in the twelfth position of the consensus Ca^{2+} binding loop in other Ca^{2+} binding proteins (CaBP) has been carried out numerous times to investigate the critical role of this highly conserved residue for the Ca^{2+}-induced conformational changes in the regulatory EF-hand proteins (Beckingham, 1991; Haiech et al., 1991; Maune et al., 1992; Carlström & Chazin, 1993; Evenäs et al., 1997). These mutations were observed to reduce drastically the affinity for Ca^{2+} in the mutated sites. Other site-specific mutagenesis studies have clearly defined these conserved Glu residues as an essential component for Ca^{2+} binding within the loops of TnC (Babu et al., 1992, 1993). The results of this study help to explain why this residue is highly conserved in the EF-hand Ca^{2+} binding proteins (Strynadka & James, 1989).

The E41A sNTnC structure stays closed in the Ca^{2+} state due to an imperfect Ca^{2+}-binding site I in which the critical bidentate Glu 41 is replaced by an Ala. Interestingly, the cNTnC structure also remains essentially closed as a result of an inactive Ca^{2+}-binding site I (Spyracopoulos et al., 1997). The 12-residue loop in the site I of cNTnC is **L**G**A**E**D**G**C**I**S**T**K**E with liganding residues as bold letters. The important Glu 40 (position 12) is present, but the first two aspartic acid residues are replaced by residues (L and A) with no Ca^{2+}-coordinating side chains, resulting in an inactive site I. In the case of E41A sNTnC, the substitution of Glu 41 by an Ala drastically reduced the Ca^{2+} binding affinity of this site but did not fully abolish the Ca^{2+} binding ability due to the effort of the remaining coordinating ligands (see above). In the case of cNTnC, the Glu 40 is present but the other ligands are not present so the Ca^{2+} cannot coordinate at all. There is therefore no Ca^{2+} for Glu 40 to interact with. The present results confirm the general belief [for a recent review, see Tobacman et al. (1996)] that there is no Ca^{2+} binding to site I. Our determined binding affinity for site II agrees well with literature values. The Ca^{2+} binding to site II of cNTnC yields ~ 7.7 kcal mol^{-1} (Table 1) of stabilizing free energy. The inactive site I in cNTnC also responds to Ca^{2+} binding to site II. This is due to the

structural coupling between the two sites. In the cTnC and cNTnC structures, we observed NOE contacts between the two loops, especially in the β-sheet. This result suggests that site I, though defunct, is not silent in the regulatory function of cTnC.

During the processes of solving the NMR structures of sTnC and sNTnC, we have noticed that these proteins dimerize and/or aggregate (Gagné et al., 1995; Slupsky et al., 1995). To assess the molecular state of E41A sNTnC in solution, we have determined the rotational correlation time (τ_{ROT}) for the protein at different $[Ca]_{total}/[E41A\ sNTnC]_{total}$ ratios as shown in Figure 6. The results clearly indicate that E41A sNTnC does not undergo a Ca^{2+}-induced dimerization/aggregation. This is consistent with the sharp NMR signals and the closed structure (Gagné et al., 1997). The sharp NMR signals and the observed closed structure for cNTnC suggest cNTnC also stays as a monomer in solution. Therefore, we conclude that our results presented in this paper are not influenced by protein dimerization/aggregation.

ACKNOWLEDGMENT

We are indebted to D. Corson and L. Golden for assistance with the protein purification, M. Carpenter for amino acid analyses, R. Boyko for his assistance with the curve fitting program, and G. McQuaid for upkeep of the NMR spectrometer. We thank S. Sia and R. Mckay for critical reading of the manuscript.

SUPPORTING INFORMATION AVAILABLE

2D $\{^1H,^{15}N\}$-HSQC spectra acquired during Ca^{2+} titration in Figure S1 for $[^{15}N]$E41A sNTnC and in Figure S2 for $[^{15}N]$cNTnC and Figure S3 showing additional examples of the Ca^{2+} titration curves as shown in Figure 2 (8 pages). Ordering information is given on any current masthead page.

REFERENCES

Anglister, J., Ren, H., Klee, C. B., & Bax, A. (1993) *J. Biol. NMR 3*, 121.
Babu, A., Su, H., Ryu, Y., & Gulati, J. (1992) *J. Biol. Chem. 267*, 15469.
Babu, A., Su, H., & Gulati, J. (1993) *Adv. Exp. Med. Biol. 332*, 125.
Beckingham, K. (1991) *J. Biol. Chem. 266*, 6027.
Bodenhausen, G., & Reuben, D. J. (1980) *Chem. Phys. Lett. 69*, 185.
Carlström, G., & Chazin, W. J. (1993) *J. Mol. Biol. 231*, 415.
Chandra, M., Dong, W.-J., Pan, B.-S., Cheung, H. C., & Solaro, R. J. (1997) *Biochemistry* (in press).
Delaglio, F., Grzesiek, S., Vuister, G. W., Zhu, G., Pfeifer, J., & Bax, A. (1995) *J. Biomol. NMR 6*, 277.
Evenäs, J., Thulin, E., Malmendal, A., Forsén, S., & Carlstrom, G. (1997) *Biochemistry 36*, 3448.
Farah, C. S., & Reinach, F. C. (1995) *FASEB J. 9*, 755.
Foguel, D., Suarez, M. C., Barbosa, C., Rodrigues, J. J., Sorenson, M. M., Smillie, L. B., & Silva, J. L. (1996) *Proc. Natl. Acad. Sci. U.S.A. 93*, 10642.
Gagné, S. M., Tsuda, S., Li, M. X., Chandra, M., Smillie, L. B., & Sykes, B. D. (1994) *Protein Sci. 3*, 1961.
Gagné, S. M., Tsuda, S., Li, M. X., Smillie, B. D., & Sykes, B. D. (1995) *Nat. Struct. Biol. 2*, 784.
Gagné, S. M., Li, M. X., & Sykes, B. D. (1997) *Biochemistry 36*, 4386.
Garrett, D. S., Powers, R., Gronenborn, A. M., & Clore, G. M. (1991) *J. Magn. Reson. 95*, 214.
Golosinska, K., Pearlstone, J. R., Borgford, T., Oikawa, K., Kay, C. M., Carpenter, M. R., & Smillie, L. B. (1991) *J. Biol. Chem. 266*, 15797.
Grabarek, Z., Tao, T., & Gergely, J. (1992) *J. Muscle Res. Cell Motil. 13*, 383.
Haiech, J., Kilhoffer, M. C., Lucas, T. J., Craig, T. A., Roberts, D. M., & Watterson, D. M. (1991) *J. Biol. Chem. 266*, 3427.
Hannon, J. D., Martyn, D. A., & Gordon, A. M. (1992) *Circ. Res. 71*, 984.
Herzberg, O., & James, M. N. G. (1988) *J. Mol. Biol. 203*, 761.
Herzberg, O., Moult, J., & James, M. N. G. (1986) *J. Biol. Chem. 261*, 2638.
Holroyde, M. J., Robertson, S. P., Johnson, J. D., Solaro, R. J., & Potter, J. D. (1980) *J. Biol. Chem. 255*, 11688.
Johnson, J. D., Collins, J. H., Robertson, S. P., & Potter, J. D. (1980) *J. Biol. Chem. 255*, 9635.
Kunkel, A. T., Roberts, J. D., & Zakour, R. A. (1987) *Methods Enzymol. 154*, 367.
Leavis, P. C., & Gergely, J. (1984) *CRC Crit. Rev. Biochem. 16*, 235.
Li, M. X., Gagné, S. M., Tsuda, S., Smillie, L. B., & Sykes, B. D. (1995) *Biochemistry 34*, 8330.
Linse, S., & Chazin, W. J. (1995) *Protein Sci. 4*, 1038.
Maune, J. F., Klee, C. B., & Beckingham, K. (1992) *J. Biol. Chem. 267*, 5286.
Mead, D. A., Skorupa, E. S., & Kemper, B. (1986) *Protein Eng. 1*, 67.
Messerle, B., Wider, G., Otting, G., Weber, C., & Wuthrich, K. (1989) *J. Magn. Reson. 85*, 608.
Potter, J. D., & Gergely, J. (1975) *J. Biol. Chem. 250*, 4628.
Putkey, J. A., Sweeney, H. L., & Campbell, S. T. (1989) *J. Biol. Chem. 264*, 12370.
Reinach, F. C., & Karlsson, R. (1988) *J. Biol. Chem. 263*, 2371.
Satyshur, K. A., Rao, S. T., Pyzalska, D., Drendel, W., Greaser, M., & Sundaralingam, M. (1988) *J. Biol. Chem. 263*, 1628.
Sheng, Z., Strauss, W. L., Francois, J. M., & Potter, J. M. (1990) *J. Biol. Chem. 265*, 21554.
Sia, S. K., Li, M. X., Spyrocoupalos, L., Gagné, S. M., Liu, W., Putkey, J. A., & Sykes, B. D. (1997) *J. Biol. Chem. 272*, 18216.
Slupsky, C. M., & Sykes, B. D. (1995) *Biochemistry 34*, 15953.
Slupsky, C. M., Kay, C. M., Reinach, F. C., Smillie, L. B., & Sykes, B. D. (1995) *Biochemistry 34*, 7365.
Spyracopoulos, L., Li, M. X., Sia, S. K., Gagné, S. M., Chandra, M., Solaro, R. J., & Sykes, B. D. (1997) *Biochemistry* (in press).
Strynadka, N. C. J., & James, M. N. G. (1989) *Annu. Rev. Biochem. 58*, 951.
Strynadka, N. C. J., Chernaia, M., Sielecki, A. R., Li, M. X., Smillie, L. B., & James, M. N. G. (1997) *J. Mol. Biol.* (in press).
Sykes, B. D., Audette, S. M., Gagné, S. M., Li, M. X., Slupsky, C. M., & Tsuda, S. (1996) in *Biomacromolecules: From 3D to Application* (Ornstein, R. L., Ed.) pp 11−19, Battelle Press, Columbus, OH.
Szczesna, D., Guzman, G., Miller, T., Zhao, J., Farokhi, K., Ellemberger, H., & Potter, J. D. (1996) *J. Biol. Chem. 271*, 8381.
Tobacman, L. S. (1996) *Annu. Rev. Physiol. 58*, 447.
Van Eerd, J. P., & Takahashi, K. (1975) *Biochem. Biophys. Res. Commun. 64*, 122.
Williams, T. C., Shelling, J. G., & Sykes, B. D. (1985) in *NATO Advance Study Institution on NMR in the Life Sciences* (Bradbury, E. M., & Nicolini, C., Eds.) pp 93−103, Plenum Press, New York.
Wimberly, B., Thulin, E., & Chazin, W. J. (1995) *Protein Sci. 4*, 1045.
Zot, A. S., & Potter, J. D. (1987) *Annu. Rev. Biophys. Biophys. Chem. 16*, 535.

BI971222L